Article type : Original Article

Reactive oxygen species generated in chloroplasts contribute to tobacco leaf infection by the necrotrophic fungus *Botrytis cinerea*

Franco R. Rossi[1,†], Adriana R. Krapp[2,†], Fabiana Bisaro[2,‡], Santiago J. Maiale[1], Fernando L. Pieckenstain[1,*] and Néstor Carrillo[2,*]

[1]*Instituto de Investigaciones Biotecnológicas-Instituto Tecnológico Chascomús Universidad Nacional de General San Martín, Consejo Nacional de Investigaciones Científicas y Técnicas (IIB-INTECH/UNSAM-CONICET), Chascomús, Argentina*

[2]*Instituto de Biología Molecular y Celular de Rosario (IBR-UNR/CONICET), Facultad de Ciencias Bioquímicas y Farmacéuticas, Universidad Nacional de Rosario (UNR), Rosario, Argentina*

[*]For correspondence (e-mails pieckenstain@intech.gov.ar and carrillo@ibr-conicet.gov.ar).

[†]F.R.R. and A.R.K. made equal contributions and are co-first authors.

[‡]Present address: Centre for Infection and Immunity, Queen's University Belfast, Belfast BT9 7AE, UK.

Running title: Chloroplastic ROS favor leaf infection by *B. cinerea*

Keywords: Chloroplastic ROS – Plant-microbe interactions – Necrotrophs – *Botrytis cinerea* – Flavodoxin – *Nicotiana tabacum*

SUMMARY

Reactive oxygen species (ROS) play fundamental roles in plant responses to pathogen infection, including modulation of cell death processes and defense-related gene expression. Cell death triggered as part of the hypersensitive response enhances resistance to biotrophic pathogens, but favors virulence of necrotrophs. Even though the involvement of ROS in the orchestration of defense responses is well established, the relative contribution of specific subcellular ROS sources to plant resistance against microorganisms with different pathogenesis strategies is not completely known. The aim of this work was to investigate the role of chloroplastic ROS in plant defense against a typical necrotrophic fungus, *Botrytis cinerea*. For this purpose, we used transgenic tobacco lines expressing a plastid-targeted cyanobacterial flavodoxin (*pfld* lines), which accumulate lower chloroplastic ROS in response to different stresses. Tissue damage and fungal growth were significantly reduced in infected leaves of *pfld* plants, as compared to infected wild-type (WT) counterparts. ROS build-up triggered by *Botrytis* infection and associated to chloroplasts was significantly decreased (70-80%) in *pfld* leaves relative to the wild type. Phytoalexin accumulation and expression of pathogenesis-related genes were induced to a lower degree in *pfld* plants than in WT siblings. The impact of fungal infection on photosynthetic activity was also lower in *pfld* leaves. The results indicate that chloroplast-generated ROS play a major role in lesion development during *Botrytis* infection. This work demonstrates that the modulation of chloroplastic ROS levels by expression of a heterologous antioxidant protein can provide a significant degree of protection against a canonical necrotrophic fungus.

INTRODUCTION

The evolution of land plants has been shaped by molecular interactions with mutualistic and pathogenic microorganisms (Chisholm *et al.*, 2006). Depending on their lifestyles and strategies of infection, plant pathogens are classified as biotrophs or necrotrophs. Biotrophs establish a long-term feeding relationship with the living cells of their hosts, without killing them, as part of the infection process. Necrotrophs, on the contrary, promote the destruction of host cells to consume their contents. A third group of pathogens, known as hemibiotrophs, exhibits both types of nutrient acquisition strategies, shifting from an initial biotrophic phase to necrotrophy at a

later stage of disease development (Laluk and Mengiste, 2010). In many instances, recognition of pathogen attack triggers a hypersensitive response (HR) in the affected tissue. The HR involves the accumulation of reactive oxygen species (ROS) and the induction of pathogenesis-related (PR) protein expression. It also promotes localized cell death (LCD) at the site of infection, which is regarded as a major factor impeding spread of biotrophic pathogens by opposing a barrier of dead cells to the invading microorganism (Glazebrook, 2005).

Contrary to biotrophs, necrotrophic pathogens are not expected to be deterred by plant cell death during the HR (Glazebrook, 2005). In fact, infection by *Botrytis cinerea*, a well-studied necrotrophic fungus that causes grey mold disease in a variety of plants, was shown to be facilitated by the onset of the HR (Govrin and Levine, 2000), and several lines of evidence suggest that this microorganism elicits the host HR on its own benefit (Govrin *et al.*, 2006; van Kan, 2006; Williamson *et al.*, 2007; Frías *et al.*, 2011; Rossi *et al.*, 2011). Challenge of bean leaves with *B. cinerea* was associated with increased ROS production at the site of attack, and these ROS were assumed to contribute to host cell death thus favoring invasion and spread of the pathogen in the dead host tissue (Tiedemann, 1997). Govrin and Levine (2000) showed that *B. cinerea* induced ROS build-up and LCD in Arabidopsis leaves, which led to rapid colonization of host tissues. Moreover, *B. cinerea* growth in Arabidopsis was enhanced by the HR caused by simultaneous infection with an avirulent bacterial strain, but suppressed in the HR-deficient mutant *dnd1*. Similar results were obtained with the closely related necrotrophic fungus *Sclerotinia sclerotiorum* (Govrin and Levine, 2000). In principle, ROS produced by the plant could be toxic for the attacking microorganism, but *B. cinerea* was shown to tolerate the oxidative burst triggered during infection of several plant species (Temme and Tudzynski, 2009). These results suggested that ROS accumulation and LCD do favor tissue colonization by necrotrophs. Other reports, however, have shown that the relationship between HR induction, ROS build-up and decreased resistance to necrotrophs is more intricate than anticipated and cannot be taken as a general rule (Malolepsza and Urbanek, 2002; Unger *et al.*, 2005; Finiti *et al*., 2014).

While the role played by ROS in the deployment of the HR is well documented, the relative contribution of the various cell sources (apoplast, mitochondria, chloroplasts, peroxisomes) is not completely clear. Several reports have shown that significant ROS production after pathogen recognition occurs in the apoplast through the action of NADPH oxidases, cell wall peroxidases and amine oxidases (Bolwell *et al.*, 2002; Marina *et al.*, 2008; Angelini *et al.*, 2010) but much less is known about the contribution of other organelles, especially plastids (Delprato *et al.*, 2015). Liu *et al.* (2007) demonstrated that chloroplast-generated-ROS contribute to a hypersensitive-like cell death process mediated by a mitogen-activated protein kinase cascade. We have recently shown that localized cell death caused by infiltration with the non-host hemibiotrophic bacterium *Xanthomonas campestris* pv. *vesicatoria* (*Xcv*) was inhibited in leaves of transgenic tobacco plants in which ROS accumulation was specifically suppressed in chloroplasts by expression of a cyanobacterial flavodoxin (Fld), indicating that plastid-generated ROS play a major role in LCD during this type of interaction (Zurbriggen *et al.*, 2009).

Fld is a flavin mononucleotide-containing electron shuttle which can mediate essentially the same reactions as the iron-sulfur protein ferredoxin (Fd), and is induced in cyanobacteria and some algae under conditions of environmental stress which cause a decline of Fd levels (Lodeyro *et al.*, 2012; Pierella Karlusich *et al.*, 2014). This flavoprotein is not found in plants (Pierella Karlusich *et al.*, 2015), but when a cyanobacterial Fld was expressed in tobacco and targeted to chloroplasts, it was able to functionally interact with plastidic enzymes, driving reducing equivalents away from oxygen and into productive oxido-reductive pathways of the chloroplast (Tognetti *et al*. 2006; Zurbriggen *et al.*, 2008). As a consequence, Fld prevented ROS build-up in plastids without affecting their production in other cellular compartments (Zurbriggen *et al.*, 2009). The resulting transgenic lines displayed increased tolerance to multiple sources of abiotic stress (Tognetti *et al*. 2006) and iron deficiency (Tognetti *et al.*, 2007), and, as indicated, exhibited little or no LCD symptoms associated with a non-host biotic interaction (Zurbriggen *et al.*, 2009).

In this article we describe the use of Fld-expressing plants to investigate the contribution of chloroplast ROS build-up to the development of disease symptoms and other plant responses during infection with a canonical necrotroph such as *B. cinerea*. We show herein that the presence of Fld did inhibit chloroplastic ROS production, tissue damage and fungal growth in leaves of transgenic tobacco lines inoculated with the pathogen. Photosynthetic activities were differentially preserved in the transformed plants. Accumulation of fluorescent phytoalexins and expression of PR genes were lower in these lines, suggesting that since *B. cinerea* infection was largely prevented by Fld, a weaker host response was elicited. The results indicate that suppression of ROS build-up in chloroplasts enhances plant resistance against necrotrophic microorganisms.

RESULTS

Flavodoxin expression in chloroplasts decreases tissue damage and hyphal growth in tobacco leaves infected with *B. cinerea*

Disease symptoms caused by *B. cinerea* are usually manifested as necrotic areas with extensive fungal growth, giving the characteristic appearance of gray mold. To examine whether chloroplastic Fld expression affects the development of leaf rot during *B. cinerea* infection, intact leaves and leaf discs obtained from two independent lines of tobacco plants expressing a plastid-targeted Fld (*pfld*5-8 and *pfld*4-2) and the corresponding wild-type (WT) parental were spot-inoculated with conidia. WT leaves exhibited some tissue discoloration around the inoculation spot 24-48 hours post-inoculation (hpi), with lesions becoming prominent 72 hpi (Figure 1a). The severity of tissue damage upon *B. cinerea* infection was significantly lower in leaves of both *pfld* lines than in their WT siblings both 48 and 72 hpi (Figure 1a, b). Experiments performed with leaf discs yielded similar results, with *pfld* tissue showing a reduction in lesion size as compared to WT discs, both 48 and 72 hpi (Figure S1).

Growth of *B. cinerea* mycelium in inoculated leaves was studied by microscopic observation after hyphal staining with Calcofluor White. In this case, conidia were spread on the surface of leaf discs with the aid of a cotton swab. The rationale behind this inoculation procedure was to facilitate further microscopic analysis by

avoiding the development of a high density of fungal mycelium in a localized spot. Hyphal growth progressed steadily in infected WT discs, but was strongly reduced in Fld-expressing plants, an effect that was already evident 24 hpi and became even more notorious 48 and 72 hpi (Figure 2a-c). Mycelial growth was inhibited by 67-90% in *pfld* lines at different post-inoculation times (Figure 2d). *B. cinerea* conidia germinated with similar efficiency (60-70%) on discs from all lines tested (Figure S2), indicating that the restriction of fungal proliferation in *pfld* plants was not due to impairment of conidia germination, but to the inhibition of mycelial growth from germinated conidia.

Flavodoxin protects photosynthetic activities during *B. cinerea* infection

Down-regulation of photosynthesis is a landmark of plant–pathogen interactions (see for instance Bilgin *et al.*, 2010), but previous results have shown that Fld expression in chloroplasts prevented this inhibition in plants infected with a hemibiotrophic bacterial pathogen (Zurbriggen *et al.*, 2009). To determine if the Fld effect on fungal colonization observed in Figures 1 and 2 was accompanied by preservation of photosynthetic activities, gas exchange and chlorophyll fluorescence were measured in *Botrytis*-infected leaves from all lines. By 48 hpi, the extent of tissue damage at the inoculation spots prevented photosynthetic determinations in this region. Therefore, measurements were carried out in asymptomatic tissues adjacent to the lesions.

Measurements of chlorophyll fluorescence were performed on dark-adapted leaves subsequently exposed to 3,500 µmol photons m^{-2} s^{-1} of actinic light (Rachoski *et al.*, 2015). WT plants infected with *B. cinerea* showed a moderate but significant decrease of the Fv/Fm ratio, which reflects photodamage to photosystem II (PSII), both 48 and 72 hpi (Figure 3a, b). The photosynthetic performance index (PI abs; Stirbet and Govindjee, 2011; see also Table S1) was determined in the same leaves used for Fv/Fm analysis. *B. cinerea* infection caused a major decline in this parameter 48 and 72 hpi in WT plants (Figure 3c, d), but exerted no effects on Fv/Fm and PI abs of *pfld* plants up to 72 hpi (Figure 3a-d). Maximal CO_2 assimilation rates (Pn) of all lines at 1,500 µmol photons m^{-2} s^{-1} (saturating light intensity) were

not affected by fungal infection 48 hpi (Figure 3e). A significant decline (~30%) was evident in WT leaves 72 hpi, as compared to mock-inoculated controls. This decline was totally prevented in *pfld* lines (Figure 3f).

Previous results have shown that Fld expression in chloroplasts resulted in increased levels of chlorophylls, carotenoids and photosynthetic activities per leaf area (Tognetti *et al.*, 2006; Ceccoli *et al.*, 2012). In agreement with those observations, both PI abs and Pn were moderately higher in mock-treated *pfld* leaves compared to the wild type (Figure 3c-f). Dissection of PSII fluorescence data indicated that *pfld* leaves contained significantly more active reaction centers (RC) per leaf cross-section (CS) than WT siblings (Figure S3a), suggesting that the extra pigments were associated, at least in part, with photosynthetic complexes. The higher RC/CS ratios caused that light exciting a fixed leaf section was distributed through more reactions centers, leading to lower photons absorbed (ABS/RC), excitons trapped (TRo/RC) and energy dissipated (DIo/RC) per active RC (Figure S3b-d). Parameters related to the efficiency of electron transfer downstream Q_A (the primary acceptor of PSII), such as ETo/CS and ψ_{Eo} (Stibert and Govindjee, 2011; Table S1), were generally higher in leaves expressing chloroplast-targeted Fld, although differences with the wild type were not statistically significant in all cases (Figure S3e, f).

Photosynthetic processes of WT plants were negatively affected by *B. cinerea* infection at various levels. Results obtained 72 hpi are shown in Figure S3. A significant fraction of reaction centers were switched off by fungal infection (Figure S3a). Photons were thus distributed in a lower number of active centers, overloading them with energy in comparison to those of mock-treated leaves. As a consequence, higher ABS/RC, TRo/RC and DIo/RC ratios were measured in inoculated WT plants (Figure S3b-d). In addition, a decrease in the ETo/CS and ψ_{Eo} values was observed (Figure S3e, f), accompanied by a decline in the quantum yield of the electron flow between Q_A and Q_B, and in the availability of electron acceptors downstream Q_A, as monitored by the ϕ_{Eo} and Sm parameters, respectively (Figure S3g, h).

The adverse effects of *Botrytis* infection were abolished in *pfld*5-8 and *pfld*4-2 leaves (Figure S3). Figure 4 provides a summary of these observations, including other photosynthetic parameters that were not affected by either pathogen or genotype, and whose relation to the photosynthetic process is briefly described in Table S1 and in more detail by Stirbet and Govindjee (2011). The pathogen-dependent declines in RC/CS, ψ_{Eo}, ϕ_{Eo}, Sm and ETo/CS and increases in ABS/RC, DIo/RC and TRo/RC in WT leaves were prevented or largely attenuated in their *pfld* counterparts (Figure 4). The collected results indicate that the presence of Fld in the two transgenic lines significantly preserved the integrity and functionality of the photosynthetic machinery in leaves infected with *B. cinerea*.

Flavodoxin decreases *Botrytis*-induced accumulation of reactive oxygen species in infected leaves

ROS build-up was visualized by 2',7'-dichlorofluorescein diacetate (DCFDA) staining of leaf discs infected with *B. cinerea* in a single spot. As indicated before, this procedure leads to high density of fungal mycelium at the inoculation site, resulting in extensive tissue destruction by 72 hpi (Figure S1). ROS-associated fluorescence was maximal in this region, and declined with the distance from the inoculation spot (Figure 5a), together with disease symptoms and hyphal growth. Given the combination of tissue damage and fungal density in the infected region, it is likely that at least part of the detected ROS were produced by *Botrytis* itself (Lyon et al., 2007). It is worth noting, in this context, that high ROS levels have been consistently observed in necrotized leaf tissues from various species upon infection with *B. cinerea*, as revealed by different labeling procedures (Simon *et al*., 2013; Finiti *et al*., 2014; López-Cruz *et al*., 2017). Both the fluorescence intensity and the extension of the fluorescent area were markedly lower in discs expressing chloroplast-targeted Fld (Figure 5a), in line with the antioxidant role reported for this flavoprotein during the non-host interaction of tobacco with *Xcv* (Zurbriggen *et al.*, 2009).

The subcellular origin of these ROS was analyzed in discs inoculated by spreading fungal conidia with a cotton swab, using DCFDA and confocal laser microscopy. Experiments in which tomato leaves were analyzed at advanced stages of infection

by *B. cinerea* revealed extensive damage in chloroplasts (Simon *et al*., 2013). ROS accumulation was therefore evaluated at a pre-symptomatic stage (22 hpi) to warrant preservation of cellular structures. Under our experimental conditions, significant ROS label was associated to chloroplasts of WT leaf-discs inoculated with *B. cinerea*, as indicated by substantial overlay of DCFDA fluorescence and chlorophyll auto-fluorescence (Figure 5b). Plastids of inoculated *pfld* discs exhibited a 70-80% decrease in ROS fluorescence, as compared to WT discs (Figure 5c, d; Figure S4).

In addition to the above-described analysis of ROS localization *in planta*, we determined ROS levels in leaf extracts obtained from asymptomatic tissues surrounding the lesions provoked by *B. cinerea* 72 hpi, using the Amplex Red probe. Fungal infection caused a 6- to 7-fold increase in ROS levels of WT leaves, while a much lower increase (4- to 5-fold) was measured in *pfld*5-8 and *pfld*4-2 extracts (Figure 5e). Importantly, ROS levels detected in mock-inoculated plants were similar for WT and *pfld* lines (Figure 5e), indicating that a constitutive reduction of ROS production in *pfld* plants was not the reason of the observed effects.

Plants expressing flavodoxin display lower accumulation of phytoalexins in response to *B. cinerea* infection

Plants usually react to the onslaught of pathogens by deploying a multigenic response that involves the synthesis of secondary metabolites and the induction of PR genes (El Oirdi *et al.*, 2010). In the case of tobacco, the phytoalexin scopoletin and its β–glycoside conjugate scopolin are known to accumulate upon infection with different microorganisms, including necrotrophic fungi such as *B. cinerea* and *Alternaria alternata* (El Oirdi *et al.*, 2010; Sun *et al.*, 2014). These coumarins display antioxidant and antimicrobial activities against a broad range of pathogens (Prats *et al.*, 2006; El Oirdi *et al.*, 2010; Sun *et al.*, 2014). Both compounds fluoresce when illuminated with UV light, and El Oirdi *et al.* (2010) have shown that most of the blue fluorescence induced in tobacco leaves upon infection with *B. cinerea* is due to the accumulation of scopoletin and scopolin.

In the present work, blue fluorescence was indeed observed around the infection zones in leaf discs from WT plants 24 hpi (Figure 6a), with both the intensity and the extension of the fluorescent regions strongly increasing by 48 hpi (Figure 6b). The blue fluorescence intensity detected 24 and 48 hpi in leaf discs from the two independent *pfld* lines was much lower than that exhibited by WT discs (Figure 6a, b), indicating that coumarin build-up was significantly reduced in Fld-expressing plants displaying a weaker *B. cinerea* infection.

Induction of defense-related genes by *B. cinerea* is attenuated in Fld-expressing plants

To determine if the expression of defense-related genes in response to *B. cinerea* infection was also affected by the presence of Fld in chloroplasts, steady-state mRNA levels of three PR genes encoding β-1,3-glucanase, chitinase and PR-1 were analyzed by real-time RT-PCR 72 hpi. *B. cinerea* infection caused a 16-fold increase in the expression of β-1,3-glucanase in WT plants, but only a 9- and 3.5-fold increase in *pfld*4-2 and *pfld*5-8 lines, respectively (Figure 7). Essentially the same behavior was observed when chitinase expression was evaluated. Upon infection, expression of this PR gene increased ~9-fold in WT plants, while only 5- and 3-fold in infected *pfld*4-2 and *pfld*5-8 lines, respectively (Figure 7). In the case of PR-1, expression was induced 8-fold by fungal infection in WT plants, but no changes were detected in infected *pfld*4-2 leaves and only a 2.5-fold increase was evident in *pfld*5-8 (Figure 7). In summary, PR gene expression induced by *B. cinerea* infection was consistently decreased in *pfld* lines exhibiting lower fungal growth.

DISCUSSION

ROS production is part of the defense machinery deployed by plants in response to infection by pathogenic microorganisms. Apart from their role in cell wall strengthening, ROS also function as second messengers that induce resistance responses such as the synthesis of pathogenesis-related proteins and phytoalexins, as well as localized cell death in tissues surrounding infection sites (Gadjev *et al.*, 2008; Zurbriggen *et al.*, 2009). Cell death processes triggered by ROS accumulation contribute to plant resistance against biotrophic microorganisms, by depriving them

from living tissues needed for successful plant colonization. This response seems not to be effective against necrotrophic pathogens, which feed on dead host tissues. In fact, the necrotrophic fungus *B. cinerea* was found to elicit host responses that lead to cell death, thus using the defensive machinery of the host on its own benefit (Govrin *et al.*, 2006). Other fungi, such as *Leptosphaeria maculans*, a hemibiotrophic pathogen of *Brassica napus*, was also found to take advantage of the oxidative burst triggered by the host plant during the necrotrophic phase, and even contribute to it (Li *et al.*, 2008; Hura *et al.*, 2014; Šašek *et al.*, 2012). The balance between ROS production and scavenging is critical for the modulation of ROS activity in both cell death promotion and signaling processes (Zurbriggen *et al.*, 2010; Baxter *et al.*, 2014). In this context, understanding the mechanisms that lead to ROS accumulation in plant tissues infected by necrotrophic fungi is of fundamental importance to provide the basis for future efforts aimed to increase plant resistance to this type of pathogens.

Plant ROS can derive from different cellular sources, such as plastids, mitochondria, peroxisomes, the cytosol and the apoplast (Tripathy and Oelmüller, 2012), but the relative contribution of each of these sources to ROS production triggered by pathogen infection is not completely clear. The role of plasma membrane-bound NADPH oxidases and class III peroxidases in ROS generation during the oxidative burst has been documented for several pathosystems (O'Brien *et al.*, 2012). However, an increasing body of evidence suggests that ROS derived from other sources also participate in defense responses (Karpinski *et al.*, 2003; Mur *et al.*, 2008). In this regard, chloroplast-generated ROS are involved in HR-like cell death processes mediated by a mitogen-activated protein kinase cascade (Liu *et al.*, 2007), and were also shown to contribute to LCD in tobacco leaves infected by the hemibiotrophic bacterium *Xcv* (Zurbriggen *et al.*, 2009). However, the role of chloroplastic ROS in plant responses to necrotrophs has not been investigated so far. Transgenic tobacco plants expressing a plastid-targeted cyanobacterial Fld accumulate lower ROS levels than WT plants in response to diverse stress factors (Tognetti *et al.*, 2006; Lodeyro *et al.*, 2016). In the present work, we used these genetically modified tobacco lines to analyze the role of chloroplastic ROS in plant responses to the necrotrophic fungus *B. cinerea*.

The reduction in lesion size exhibited by *pfld* leaves compared to their WT counterparts (Figure 1, Figure S1) suggests that chloroplastic ROS contribute to leaf damage during fungal infection. By using ROS-generating enzymes as well as catalase and NADPH oxidase inhibitors, Govrin and Levine (2000) have shown that ROS accumulation was involved in the development of necrotic lesions in Arabidopsis leaves infected with *B. cinerea* or *S. sclerotiorum*. Conversely, suppression of ROS build-up is part of the protective mechanisms triggered by the resistance priming inducer hexanoic acid in tomato leaves against *B. cinerea* infection (Finiti *et al*., 2014). These observations fully agree with our own, although Finiti *et al*. (2014) did not identify the cellular source(s) of ROS affected by hexanoic acid in their experiments. Within this context, the present work provides evidence that leaf rot caused by *B. cinerea* depends, at least in part, on the generation of ROS by the chloroplastic machinery. ROS have been reported to accumulate in various cellular compartments during *Botrytis* infection (Simon *et al*., 2013). Confocal microscopy analysis showed chloroplast labeling by a ROS-dependent probe in infected WT tissue (Figure 5b-d), although staining of other organelles such as mitochondria and peroxisomes cannot be ruled out by this procedure. Interestingly, the reduction in lesion size exhibited by *pfld* lines was associated with impaired growth of fungal mycelium even before full manifestation of disease symptoms (24 hpi, Figure 2), and several experimental approaches demonstrated that a reduction of chloroplastic ROS was evident in *pfld* lines at this stage (Figure 5; Figure S4). In conjunction, these observations suggest that production of chloroplastic ROS contributes to tissue damage at early stages of infection.

It is worth noting that lesion development was only partially reduced in *pfld* lines, indicating that chloroplastic ROS were not the only factor determining tissue damage. It should be kept in mind that as a necrotroph, *B. cinerea* deploys multiple strategies to promote host cell death (van Kan, 2006), and interfering with one of them only leads to a partial reduction of virulence. Moreover, cellular ROS sources other than chloroplasts can probably contribute to maintain a certain degree of virulence during infection of *pfld* lines with the fungus.

NADPH-consuming reactions involved in different chloroplastic metabolic pathways, including the Calvin cycle, are early targets of inhibition by different stresses. Along with the decrease in Fd expression that occurs under stress conditions (Tognetti *et*

al., 2006; Zurbriggen *et al.*, 2009; Pierella Karlusich *et al.*, 2017), this leads to the accumulation of NADPH, limitation of physiological acceptors (oxidized Fd and $NADP^+$), and as a consequence, over-reduction of intermediate components of the photosynthetic electron transfer chain (PETC) in the thylakoid membrane. Under these conditions, electron transfer to alternative acceptors such as oxygen leads to the generation of ROS and in turn, oxidative stress and further inhibition of photosynthesis, initiating a self-propagating process of ROS production and cell damage (Tognetti *et al.*, 2006). Fld, when present, can disrupt this vicious cycle by acting as an efficient electron acceptor in place of Fd, and redirecting reducing equivalents away from oxygen and into productive electron-consuming pathways of the chloroplast (Zurbriggen *et al*., 2008; Lodeyro *et al*., 2012). By doing so, Fld not only limits ROS propagation in chloroplasts but also relieves the excitation pressure on the PETC.

In the present work, photosynthetic parameters of WT plants were affected by *B. cinerea* infection at various levels (Figure 3, 4; Figure S3; Table S1), most conspicuously by decreasing the fraction of active reaction centers per illuminated leaf cross-sections (Figure 4; Figure S3a). This inactivation led, in turn, to overloading of PSII reaction centers with light energy (Figure S3b-d), lower photosynthetic efficiency (Figure S3e-h), and reduction of CO_2 assimilation rates (Figure 3). All these symptoms were significantly alleviated by Fld expression in chloroplasts (Figure 3, 4; Figure S3; Table S1). This finding, along with the decrease in ROS accumulation exhibited by the transgenic lines (Figure 5), indicates that Fld expression in chloroplasts contributes to sustain the photosynthetic electron flow during *B. cinerea* infection, thus attenuating the adverse effects of this stress condition on the photosynthetic machinery.

ROS were initially regarded only as toxic by-products of aerobic metabolism, but it is now accepted that they play a crucial role in signaling, modulating growth, development, stress responses and cell death programs (Apel and Hirt, 2004; Foyer *et al*., 2017). During plant responses to pathogen infection, ROS participate in the regulation of defense-related gene expression, both locally and systemically (Baxter *et al.*, 2014). In the present work, we found that induction of defense-related genes in asymptomatic tissues adjacent to the lesions provoked by *B. cinerea* was attenuated in *pfld* lines (Figure 7). Similarly, *B. cinerea* induction of phytoalexin accumulation

was lower in infected *pfld* leaves than in their WT counterparts (Figure 6). It is worth noting that this attenuation of defense responses did not exert a negative impact on disease resistance. Moreover, as discussed previously, resistance to *B. cinerea* infection was in fact higher in *pfld* lines than in WT plants (Figure 1, 2). Lower ROS levels in Fld-expressing leaves limited tissue damage (Figure 1, Figure S1), restricting the access of *B. cinerea* to nutrients and inhibiting its spread (Figure 2), which represents an increase in disease resistance. We propose that this effect explains why *pfld* plants deployed a less intense response (to a weaker infection), as reflected by lower accumulation of phytoalexins and decreased induction of PR-encoding genes (Figure 6, 7).

In conclusion, our results indicate that chloroplastic ROS play an important role in *B. cinerea* virulence in this host plant. This work also demonstrates that expression of a cyanobacterial Fld in chloroplasts, which can functionally replace the cognate electron transfer protein Fd, significantly decreased chloroplastic ROS accumulation in response to infection and enhanced tobacco resistance to *B. cinerea*. In this way, modulation of chloroplastic ROS production by means of expressing this alternative electron carrier represents a promising strategy to increase plant resistance to infection by a typical necrotrophic fungus.

EXPERIMENTAL PROCEDURES

Plant lines and *B. cinerea* strains

Preparation and characterization of homozygous nuclear-transformed tobacco plants (*Nicotiana tabacum* cv *Petit Havana*) expressing a plastid-targeted Fld have been described previously (Tognetti *et al.*, 2006). Independent lines *pfld*4-2 and *pfld*5-8 accumulate similar levels of Fld in chloroplasts (60-70 pmol g^{-1} of fresh leaf weight), in the same order of endogenous Fd. WT and *pfld* plants were grown at 250 µmol photons m^{-2} s^{-1} and 24 ± 1 ºC, with a 16-h photoperiod during 6-8 weeks prior to use.

The *B. cinerea* strain used in this study was B05.10, and was routinely maintained on potato dextrose agar supplemented with 40 mg mL^{-1} of tomato leaf powder at 22 ºC and sub-cultured biweekly (Flors *et al.*, 2007).

Isolation of *B. cinerea* conidia

Conidia were collected from 7- to 10-days-old colonies with sterile water containing 0.02% (v/v) Tween-20. The suspension was filtered through a cotton layer to eliminate mycelium debris, and conidia were collected by centrifugation (15 min at 1,900 x*g*), washed twice with 1 mL of sterile water, and finally re-suspended in potato dextrose broth supplemented with 10 mM potassium phosphate and 10 mM sucrose (KPS). Conidia were counted in a Neubauer chamber and their concentrations adjusted to 1 x 10^5 conidia mL^{-1}. Prior to plant inoculation, conidial suspensions were incubated for 3 h at 25 ºC without shaking, and subsequently diluted to the appropriate concentration for each experiment, as indicated in the corresponding Legends to Figures.

Plant inoculation

Leaves were inoculated with conidial suspensions as indicated for each experiment, either in single spots (10 µL) on each side of the main vein of attached leaves, or in the center of leaf discs. Alternatively, leaf discs were inoculated by spreading 10 µL of the indicated concentration of fungal conidia with a cotton swab embedded in KPS. In all cases, conidia were applied on the adaxial surface of leaves or leaf discs. Mock inoculations were carried out with the same volumes of KPS. To obtain saturating humidity conditions, leaf discs were incubated in Petri dishes containing 0.8% (w/v) agar-water, whereas whole plants were placed inside a clear plastic box at 22 ºC. Illumination at 250 µmol photons m^{-2} s^{-1} was provided by fluorescent white lights under a 16-h photoperiod. At the times indicated, leaves and discs were photographed with a Canon SX50 Hs camera. Lesion areas were measured using the Image Pro Plus V4.1 software.

Colonization of host tissues by fungal mycelium

Growth of *B. cinerea* mycelium on plant tissues was analyzed by epifluorescence microscopy in *pfld* and WT plants at different times after inoculation of leaf discs with the cotton swab procedure. Fungal hyphae were stained by vacuum-infiltrating inoculated discs with 0.1% (w/v) Calcofluor White (Fluorescent brightener from Sigma) in 10% (w/v) KOH. Stained hyphae were visualized as a strong blue-white

fluorescence in an Olympus BH2 microscope at an excitation wavelength of 360-390 nm and an emission wavelength of 420-460 nm (Harrington and Hageage, 1991). Photographs were taken with a Nikon Digital Sight DS-Fi1 camera coupled to the microscope at different times after inoculation with *B*. *cinerea*, and images were analyzed using the Image J software.

For germination studies, leaf discs were inoculated in a single spot of 10 µL (10^3 conidia) and incubated for 3 h at 25 ºC. Conidia were subsequently stained with Calcofluor White and analyzed as described above.

ROS determinations

Hydrogen peroxide was measured in cleared leaf extracts using the Amplex Red method (Molecular Probes) by quantifying the red fluorescent product (resorufin), according to the manufacturer´s instructions. Asymptomatic tissue (40-60 mg per leaf) surrounding (4-5 mm) the lesions developed on leaves spot-inoculated with fungal conidia was harvested and ground under liquid N_2 with a mortar and pestle. The powder thus obtained (50 mg) was resuspended in 500 µL of 50 mM KH_2PO_4, pH 7.4, and centrifuged for 15 min at 13,000 *x g*. Then, 100 µL of the supernatant were transferred to a 96-well clear bottom black microplate and supplemented with Amplex Red and horseradish peroxidase to a final concentration of 100 µM and 0.2 U mL^{-1}, respectively. Samples were incubated at 37 ºC for 30 min and the fluorescence was read (560_{Ex} – 590_{Em}) in a multi-mode microplate reader (BioTek, Synergy H1 Hybrid Reader).

ROS accumulation was visualized as green fluorescence on spot-inoculated leaf discs (72 hpi) with an Olympus MVX10 Macro Zoom Fluorescence Microscope. Discs were vacuum-infiltrated in the dark with 1 mL of 50 µM DCFDA in 10 mM Tris-HCl, pH 7.5. Subcellular location of ROS 22 hpi was analyzed in discs inoculated by spreading 10 µL of a suspension containing 1 x 10^4 conidia mL^{-1}. Discs were stained with DCFDA as indicated above and ROS were visualized in an Eclipse TE–2000–E2 Nikon confocal microscope with excitation at 488 nm and emission at 515-530 nm. Fluorescence intensities were quantified using the Image J software.

Detection of scopoletin and related compounds

Leaf discs were spot-inoculated with *B. cinerea* conidia, incubated for 24-48 h and then exposed to UV light (~302 nm). Images were taken with a Canon SX50 Hs camera. Fluorescence intensities were quantified with the Image J software.

Photosynthetic parameters

Chlorophyll fluorescence fast-transients of PSII were measured in asymptomatic leaf areas surrounding the infection spots (4-5 mm from the borders of the lesions) with a non-invasive fluorometer (Pocket PEA, Hansatech Instruments®). Dark-adapted leaves were obtained by covering them with a leaf clip during 20 min. Clips were then opened and chlorophyll fluorescence was measured by exposing the leaves to a 3-s saturating light pulse of 3,500 µmol photons m^{-2} s^{-1} (Rachoski *et al.*, 2015). Photosynthetic parameters were calculated according to Stirbet and Govindjee (2011).

Maximal CO_2 assimilation rates were measured using a portable photosynthesis system (TPS-2, MA, USA). The gas exchange parameter (net photosynthesis, Pn) was determined in asymptomatic leaf areas surrounding the infection spots at 1,500 µmol photons m^{-2} s^{-1} (von Caemmerer and Farquhar, 1981).

RNA isolation and real time RT-PCR

RNA was extracted from asymptomatic leaf areas surrounding the infection spots of leaves using Trizol (Invitrogen), and contaminating DNA was removed with Turbo™ RNase-free DNase (AMBION, Life Technologies). First strand cDNA was synthesized from 1 µg of total RNA with M-MLV reverse transcriptase (Life Technologies) and oligo(dT) primers. Real time RT-PCR was performed with Fast Start Universal SYBR Green Master (with ROX) (Roche) and gene-specific primers (Table S2). The tobacco gene coding for elongation factor 1α (EF1α) was used as reference gene for data normalization (Schmidt and Delaney, 2010).

Statistical analyses

Results are expressed as means ± SD. Data presented are representative of at least three similar experiments. Lesion areas, hyphal growth and scopoletin accumulation were analyzed by one-way ANOVA and Dunnett's post-test. Photosynthetic parameters and CO_2 assimilation rates were analyzed by two-way ANOVA and Tukey´s post-test. ROS levels estimated by DCFDA staining and the Amplex Red method were analyzed by two-way ANOVA and Bonferroni's post-test. Real time RT-PCR results were analyzed with the REST software 2.0.7 (Pfaffl *et al.*, 2002).

ACKNOWLEDGEMENTS

We are indebted to P. A. Uchiya (IIB-INTECH) and R. Vena (IBR) for technical assistance. This work was supported by grants PICT 2012-2851, PICT 2012-1716 and PICT 2014-3286 from the National Agency for the Promotion of Science and Technology (ANPCyT, Argentina), NC and ARK are Faculty members of the School of Biochemical and Pharmaceutical Sciences, University of Rosario (Facultad de Ciencias Bioquímicas y Farmacéuticas, Universidad Nacional de Rosario, Argentina). FRR, ARK, SJM, FLP and NC are staff researchers of the National Research Council (CONICET, Argentina). The authors declare no conflict of interest.

SHORT SUPPORTING INFORMATION LEGENDS

Figure S1. Disease symptoms caused by *B. cinerea* infection in leaf discs of WT and transgenic *pfld* lines.

Figure S2. Germination of *B. cinerea* conidia on leaf discs of WT and *pfld* lines.

Figure S3. OJIP test parameters of WT and *pfld* plants infected by *B. cinerea*.

Figure S4. ROS levels in WT and Fld-expressing leaves infected with *B. cinerea*.

Table S1. Summary of the OJIP test formulae.

Table S2. Primers used for real time RT-PCR.

REFERENCES

Angelini, R., Cona, A., Federico, R., Fincato, P., Tavladoraki, P. and Tisi, A. (2010) Plant amine oxidases “on the move”: an update. *Plant Physiol. Biochem.* **48**, 560–564.

Apel, K. and Hirt, H. (2004) Reactive oxygen species: metabolism, oxidative stress, and signal transduction. *Annu. Rev. Plant Biol.* **55**, 373–399.

Baxter, A., Mittler, R. and Suzuki, N. (2014) ROS as key players in plant stress signalling. *J. Exp. Bot.* **65**, 1229–1240.

Bilgin, D.D., Zavala, J.A., Zhu, J., Clough, S.J., Ort, D.R. and DeLucia, E.H. (2010) Biotic stress globally downregulates photosynthesis genes. *Plant Cell Environ.* **33**, 1597–1613.

Bolwell, G.P., Bindschedler, L. V, Blee, K.A., Butt, V.S., Davies, D.R., Gardner, S.L., Gerrish, C. and Minibayeva, F. (2002) The apoplastic oxidative burst in response to biotic stress in plants: a three-component system. *J. Exp. Bot.* **53**, 1367–1376.

Ceccoli, R.D., Blanco, N.E., Segretin, M.E., Melzer, M., Hanke, G.T., Scheibe, R., Hajirezaei, M.R., Bravo-Almonacid, F.F. and Carrillo, N. (2012) Flavodoxin displays dose-dependent effects on photosynthesis and stress tolerance when expressed in transgenic tobacco plants. *Planta*, **236**, 1447–1458.

Chisholm, S.T., Coaker, G., Day, B. and Staskawicz, B.J. (2006) Host-microbe interactions: shaping the evolution of the plant immune response. *Cell*, **124**, 803–814.

Delprato, M.L., Krapp, A.R. and Carrillo, N. (2015) Green light to plant responses to pathogens: the role of chloroplast light-dependent signaling in biotic stress. *Photochem. Photobiol.* **91**, 1004–1011.

El Oirdi, M., Trapani, A. and Bouarab, K. (2010) The nature of tobacco resistance against *Botrytis cinerea* depends on the infection structures of the pathogen. *Environ. Microbiol.* **12**, 239–253.

Finiti, I., Leyva, M.O., Vicedo, B., Gómez-Pastor, R., López-Cruz, J., García-Agustín, P., Real, M.D. and González-Bosch, C. (2014) Hexanoic acid protects tomato plants against *Botrytis cinerea* by priming defence responses and reducing oxidative stress. *Mol. Plant Pathol.* **15**, 550-562.

Flors, V., Leyva, M.O., Vicedo, B., Finiti, I., Real, M.D., García-Agustín, P., Bennett, A.B. and González-Bosch, C. (2007) Absence of the endo-β-1,4-glucanases Cel1 and Cel2 reduces susceptibility to *Botrytis cinerea* in tomato. *Plant J.* **52**, 1027–1040.

Foyer, C.H., Ruban, A.V. and Noctor, G. (2017) Viewing oxidative stress through the lens of oxidative signalling rather than damage. *Biochem. J.* **474**, 877–883.

Frías, M., González, C. and Brito, N. (2011) BcSpl1, a cerato-platanin family protein, contributes to *Botrytis cinerea* virulence and elicits the hypersensitive response in the host. *New Phytol.* **192**, 483–495.

Gadjev, I., Stone, J.M. and Gechev, T.S. (2008) Programmed cell death in plants: new insights into redox regulation and the role of hydrogen peroxide. *Int. Rev.*

Cell Mol. Biol. **270**, 87–144.

Glazebrook, J. (2005) Contrasting mechanisms of defense against biotrophic and necrotrophic pathogens. *Annu. Rev. Phytopathol.* **43**, 205–227.

Govrin, E.M. and Levine, A. (2000) The hypersensitive response facilitates plant infection by the necrotrophic pathogen *Botrytis cinerea*. *Curr. Biol.* **10**, 751–757.

Govrin, E.M., Rachmilevitch, S., Tiwari, B.S., Solomon, M. and Levine, A. (2006) An elicitor from *Botrytis cinerea* induces the hypersensitive response in *Arabidopsis thaliana* and other plants and promotes the gray mold disease. *Phytopathology*, **96**, 299–307.

Harrington, B.J. and Hageage, G.J. (1991) Calcofluor white: tips for improving its use. *Clin. Microbiol. Newsl.* **13**, 3–5.

Hura, K., Hura, T., Bączek-Kwinta, R., Grzesiak, M. and Płażek, A. (2014) Induction of defense mechanisms in seedlings of oilseed winter rape inoculated with *Phoma lingam* (*Leptosphaeria maculans*). *Phytoparasitica*, **42**, 145–154.

Karpinski, S., Gabrys, H., Mateo, A., Karpinska, B. and Mullineaux, P.M. (2003) Light perception in plant disease defence signalling. *Curr. Opin. Plant Biol.* **6**, 390–396.

Laluk, K. and Mengiste, T. (2010) Necrotroph attacks on plants: wanton destruction or covert extortion? *Arabidopsis Book*, **8**, e0136.

Li, H., Sivasithamparam, K., Barbetti, M.J., Wylie, S.J. and Kuo, J. (2008) Cytological responses in the hypersensitive reaction in cotyledon and stem tissues of *Brassica napus* after infection by *Leptosphaeria maculans*. *J. Gen. Plant Pathol.* **74**, 120–124.

Liu, Y., Ren, D., Pike, S., Pallardy, S., Gassmann, W. and Zhang, S. (2007) Chloroplast-generated reactive oxygen species are involved in hypersensitive response-like cell death mediated by a mitogen-activated protein kinase cascade. *Plant J.* **51**, 941–954.

Lodeyro, A.F., Ceccoli, R.D., Pierella Karlusich, J.J. and Carrillo, N. (2012) The importance of flavodoxin for environmental stress tolerance in photosynthetic microorganisms and transgenic plants. Mechanism, evolution and biotechnological potential. *FEBS Lett.* **586**, 2917–2924.

Lodeyro, A.F., Giró, M., Poli, H.O., Bettucci, G., Cortadi, A., Ferri, A.M. and Carrillo, N. (2016) Suppression of reactive oxygen species accumulation in chloroplasts prevents leaf damage but not growth arrest in salt-stressed tobacco plants. *PLoS One*, **11**, e0159588.

López-Cruz, J., Crespo-Salvador, Ó., Fernández-Crespo, E., García Agustín, P. and González-Bosch, C. (2017) Absence of Cu-Zn superoxide dismutase BCSOD1 reduces *Botrytis cinerea* virulence in Arabidopsis and tomato plants, revealing interplay among reactive oxygen species, callose and signalling pathways. *Mol Plant Pathol.* **18**, 16–31.

Lyon, G.D., Goodman, B.A. and Williamson, B. (2007) *Botrytis cinerea* perturbs redox processes as an attack strategy in plants. In Botrytis*: Biology, Pathology and Control* (Elad, Y., Williamson, B., Tudzynski, P. and Delen, N., eds). Dordrecht: Springer, Dordrecht, pp. 119–141.

Malolepsza, U. and Urbanek, H. (2002) *o*-Hydroxyethylorutin-mediated enhancement of tomato resistance to *Botrytis cinerea* depends on a burst of reactive oxygen species. *J. Phytopathol.* **150**, 616–624.

Marina, M., Maiale, S.J., Rossi, F.R., Romero, M.F., Rivas, E.I., Gárriz, A., Ruiz, O.A. and Pieckenstain, F.L. (2008) Apoplastic polyamine oxidation plays different roles in local responses of tobacco to infection by the necrotrophic fungus *Sclerotinia sclerotiorum* and the biotrophic bacterium *Pseudomonas viridiflava*. *Plant Physiol.* **147**, 2164–2178.

Mur, L.A.J., Kenton, P., Lloyd, A.J., Ougham, H. and Prats, E. (2008) The hypersensitive response; the centenary is upon us but how much do we know? *J. Exp. Bot.* **59**, 501–520.

O'Brien, J.A., Daudi, A., Butt, V.S. and Bolwell, G.P. (2012) Reactive oxygen species and their role in plant defence and cell wall metabolism. *Planta*, **236**, 765–779.

Pfaffl, M.W., Horgan, G.W. and Dempfle, L. (2002) Relative expression software tool (REST) for group-wise comparison and statistical analysis of relative expression results in real-time PCR. *Nucleic Acids Res.* **30**, e36.

Pierella Karlusich, J.J., Lodeyro, A.F. and Carrillo, N. (2014) The long goodbye: the rise and fall of flavodoxin during plant evolution. *J. Exp. Bot.* **65**, 5161–5178.

Pierella Karlusich, J.J., Ceccoli, R.D., Graña, M., Romero, H. and Carrillo, N. (2015) Environmental selection pressures related to iron utilization are involved in the loss of the flavodoxin gene from the plant genome. *Genome Biol. Evol.* **7**, 750–767.

Pierella Karlusich, J.J., Zurbriggen, M.D., Shahinnia, F., Sonnewald, S., Sonnewald, U., Hosseini, S.A., Hajirezaei, M.R. and Carrillo, N. (2017) Chloroplast redox status modulates genome-wide plant responses during the non-host interaction of tobacco with the hemibiotrophic bacterium *Xanthomonas campestris* pv. *vesicatoria*. *Front. Plant Sci.* **8**, 1158. doi: 10.3389/fpls.2017.01158.

Prats, E., Bazzalo, M.E., León, A. and Jorrín, J. V. (2006) Fungitoxic effect of scopolin and related coumarins on *Sclerotinia sclerotiorum*. A way to overcome sunflower head rot. *Euphytica*, **147**, 451–460.

Rachoski, M., Gázquez, A., Calzadilla, P., Bezus, R., Rodríguez, A., Ruiz, O.A., Menéndez, A.B. and Maiale, S. (2015) Chlorophyll fluorescence and lipid peroxidation changes in rice somaclonal lines subjected to salt stress. *Acta Phisiologia Plant.* **37**, 1–12.

Rossi, F.R., Gárriz, A., Marina, M., Romero, F.M., González, M.E., Collado, I.G. and Pieckenstain, F.L. (2011) The sesquiterpene botrydial produced by *Botrytis cinerea* induces the hypersensitive response on plant tissues and its action is modulated by salicylic acid and jasmonic acid signaling. *Mol. Plant-Microbe Interact.* **24**, 888–896.

Šašek, V., Nováková, M., Jindřichová, B., Bóka, K., Valentová, O. and Burketová, L. (2012) Recognition of avirulence gene *AvrLm1* from hemibiotrophic ascomycete *Leptosphaeria maculans* triggers salicylic acid and ethylene signaling in *Brassica napus*. *Mol. Plant-Microbe Interact.* **25**, 1238–

1250.

Schmidt, G.W. and Delaney, S.K. (2010) Stable internal reference genes for normalization of real-time RT-PCR in tobacco (*Nicotiana tabacum*) during development and abiotic stress. *Mol. Genet. Genomics*, **283**, 233–241.

Simon, U.K., Polanschütz, L.M., Koffler, B.E. and Zechmann, B. (2013) High resolution imaging of temporal and spatial changes of subcellular ascorbate, glutathione and H_2O_2 distribution during *Botrytis* cinerea infection in Arabidopsis. *PLoS One*, **8**, e65811.

Stirbet, A. and Govindjee (2011) On the relation between the Kautsky effect (chlorophyll *a* fluorescence induction) and Photosystem II: basics and applications of the OJIP fluorescence transient. *J. Photochem. Photobiol. B Biol.* **104**, 236–257.

Sun, H., Hu, X., Ma, J., Hettenhausen, C., Wang, L., Sun, G., Wu, J. and Wu, J. (2014) Requirement of ABA signalling-mediated stomatal closure for resistance of wild tobacco to *Alternaria alternata*. *Plant Pathol.* **63**, 1070–1077.

Temme, N. and Tudzynski, P. (2009) Does *Botrytis cinerea* ignore H_2O_2-induced oxidative stress during infection? Characterization of *Botrytis* activator protein 1. *Mol. Plant-Microbe Interact.* **22**, 987–998.

Tiedemann, A.V. (1997) Evidence for a primary role of active oxygen species in induction of host cell death during infection of bean leaves with *Botrytis cinerea*. *Physiol. Mol. Plant Pathol.* **50**, 151–166.

Tognetti, V.B., Palatnik, J.F., Fillat, M.F., Melzer, M., Hajirezaei, M.R., Valle, E.M. and Carrillo, N. (2006) Functional replacement of ferredoxin by a cyanobacterial flavodoxin in tobacco confers broad-range stress tolerance. *Plant Cell*, **18**, 2035–2050.

Tognetti, V.B., Zurbriggen, M.D., Morandi, E.N., Fillat, M.F., Valle, E.M., Hajirezaei, M.R. and Carrillo, N. (2007) Enhanced plant tolerance to iron starvation by functional substitution of chloroplast ferredoxin with a bacterial flavodoxin. *Proc. Natl. Acad. Sci. USA*, **104**, 11495–11500.

Tripathy, B.C. and Oelmüller, R. (2012) Reactive oxygen species generation and signaling in plants. *Plant Signal. Behav.* **7**, 1621–1633.

Unger, C., Kleta, S., Jandl, G. and Tiedemann, A.V. (2005) Suppression of the defence-related oxidative burst in bean leaf tissue and bean suspension cells by the necrotrophic pathogen *Botrytis cinerea*. *J. Phytopathol.* **153**, 15–26.

Van Kan, J.A.L. (2006) Licensed to kill: the lifestyle of a necrotrophic plant pathogen. *Trends Plant Sci.* **11**, 247–253.

Von Caemmerer, S. and Farquhar, G.D. (1981) Some relationships between the biochemistry of photosynthesis and the gas exchange of leaves. *Planta*, **153**, 376–387.

Williamson, B., Tudzynski, B., Tudzynski, P. and van Kan, J.A.L. (2007) *Botrytis cinerea*: the cause of grey mould disease. *Mol. Plant Pathol.* **8**, 561–580.

Zurbriggen, M.D., Tognetti, V.B., Fillat, M.F., Hajirezaei, M.R., Valle, E.M. and Carrillo, N. (2008) Combating stress with flavodoxin: a promising route for crop improvement. *Trends Biotechnol.* **26**, 531–537.

Zurbriggen, M.D., Carrillo, N., Tognetti, V.B., Melzer, M., Peisker, M., Hause, B. and Hajirezaei, M.R. (2009) Chloroplast-generated reactive oxygen species play a major role in localized cell death during the non-host interaction between tobacco and *Xanthomonas campestris* pv. *vesicatoria*. *Plant J.* **60**, 962–973.

Zurbriggen, M.D., Carrillo, N. and Hajirezaei, M.R. (2010) ROS signaling in the hypersensitive response. When, where and what for? *Plant Signal. Behav.* **5**, 393–396.

FIGURES LEGENDS

Figure 1. Tissue damage caused by *B. cinerea* infection in WT and transgenic *pfld* lines. Leaves were inoculated with 10 µL of a suspension containing 2.5 x 10^4 conidia on each side of the central vein. (a) Disease symptoms 72 hpi. (b) Sizes of the lesions around the inoculation sites were determined 48 hpi (left) and 72 hpi (right). Results are the means of 5 to 7 replicate leaves ± SD, and statistically significant differences between transgenic and WT plants according to one-way ANOVA and post-hoc comparisons by Dunnet's test are indicated as * ($P \leq 0.05$) and ** ($P \leq 0.01$).

Figure 2. Growth of *B. cinerea* mycelium on leaf discs of WT and *pfld* lines. Discs were inoculated by spreading 10 µL of a suspension containing 1 x 10^5 conidia mL^{-1} with a cotton swab on the adaxial surface. (a-c) Hyphal staining with Calcofluor White 24 hpi (a), 48 hpi (b) and 72 hpi (c) as analyzed by epifluorescence microscopy. Bars = 10 µm. (d) Mycelial growth 24, 48 and 72 hpi. Blue fluorescence intensity is expressed in arbitrary units (AU). Results are means of 3 replicate discs ± SD, and statistically significant differences between transgenic and WT plants according to one-way ANOVA and post-hoc by Dunnett's test are indicated as *** ($P \leq 0.001$).

Figure 3. Photosynthetic activities of WT and *pfld* lines infected by *B. cinerea*. Attached leaves were inoculated with 10 µL of a suspension containing 2.5 x 10^4 conidia mL^{-1} on each side of the central vein and plants were incubated during the indicated time-periods within clear plastic boxes to obtain high humidity. Chlorophyll fluorescence parameters were determined in asymptomatic tissues surrounding the lesions (4-5 mm). The maximum quantum efficiency of PSII (Fv/Fm) (a, b), the performance index (PI abs) (c, d) and the maximal CO_2 assimilation rate (net

photosynthesis = Pn) (e, f) were measured 48 and 72 hpi. White and black bars represent mock- and *B. cinerea*-inoculated plants, respectively. Results are means of 4-5 replicate leaves ± SD, and different letters indicate statistically significant differences ($P \leq 0.05$) between control and infected plants according to two-way ANOVA and Tukey´s post-test.

Figure 4. Radar charts of OJIP test parameters determined in WT and *pfld* lines infected with *B. cinerea*. Attached leaves from WT (a), *pfld*4-2 (b) and *pfld*5-8 (c) plants were spot-inoculated with 10 µL of a suspension containing 2.5 x 10^4 conidia mL^{-1} on each side of the central vein and plants were incubated within clear plastic boxes to obtain high humidity. OJIP test parameters were measured in asymptomatic tissues surrounding the lesions 72 hpi. Mean values of 12 OJIP parameters are shown in radar charts for mock (blue lines) and infected (red lines) leaves. Definition of each parameter is provided in Table S1.

Figure 5. Reactive oxygen species (ROS) accumulation in WT and *pfld* lines infected by *B. cinerea*. *In planta* ROS accumulation was analyzed by fluorescence microscopy after tissue infiltration with DCFDA (a-d). (a) Fluorescence microscopy analysis of ROS accumulation in leaf discs 72 h after spot-inoculation with 10 µL of a suspension containing 2.5 x 10^4 conidia mL^{-1}. Bar = 1 mm. (b-d) Confocal microscopy analysis of subcellular ROS location. Leaf discs were inoculated by spreading 10 µL of a 1 x 10^4 conidia mL^{-1} suspension with a cotton swab. Images show chlorophyll autofluorescence, ROS fluorescence and a merge of chlorophyll and ROS fluorescence for WT (b), *pfld4-2* (c) and *pfld5-8* (d) lines 22 hpi. Bars = 10 µm. (e) Quantification of hydrogen peroxide levels in whole leaf tissue. Leaves were spot-inoculated with 10 µL of a suspension containing 2.5 x 10^4 conidia mL^{-1} on both sides of the central vein and incubated for 72 h. Hydrogen peroxide levels in leaf extracts obtained from tissues adjacent to lesions (4-5 mm) were quantified using the Amplex Red probe. White and black bars represent mock- and *B. cinerea*-inoculated plants, respectively. Results are means of 5 replicate leaves ± SD and different letters indicate statistically significant differences ($P \leq 0.05$) according to two-way ANOVA and Bonferroni's multiple comparison test.

Figure 6. Phytoalexin accumulation in leaf discs of WT and transgenic *pfld* lines infected with *B. cinerea*. Leaf discs were spot-inoculated with 10 µL of a suspension containing 1 x 10^5 conidia mL^{-1} on the adaxial surface. Panels on the left show blue

fluorescence due to the accumulation of scopoletin and related compounds in inoculated discs 24 hpi (a) and 48 hpi (b). Panels on the right show the results of fluorescence intensity quantification with the Image J software 24 hpi (a) and 48 hpi (b). Results are means of 5 replicate discs ± SD, and statistically significant differences between control and infected transgenic plants according to one-way ANOVA and Dunnett's test are indicated as *** ($P \leq 0.001$).

Figure 7. Expression of defense-related genes in WT and *pfld* lines infected by *B. cinerea*. Droplets (10 µL) of a suspension containing 2.5 x 10^4 conidia mL^{-1} were spot-inoculated on both sides of the central vein and real-time RT-PCR was used to analyze the abundance of gene transcripts 72 hpi. The expression of each gene was normalized to its expression in mock-inoculated plants. Results are means ± SD of 5 replicates and statistically significant differences in gene expression between inoculated and non-inoculated plants of the same line are shown as: * ($P \leq 0.05$), ** ($P \leq 0.01$) and *** ($P \leq 0.001$).

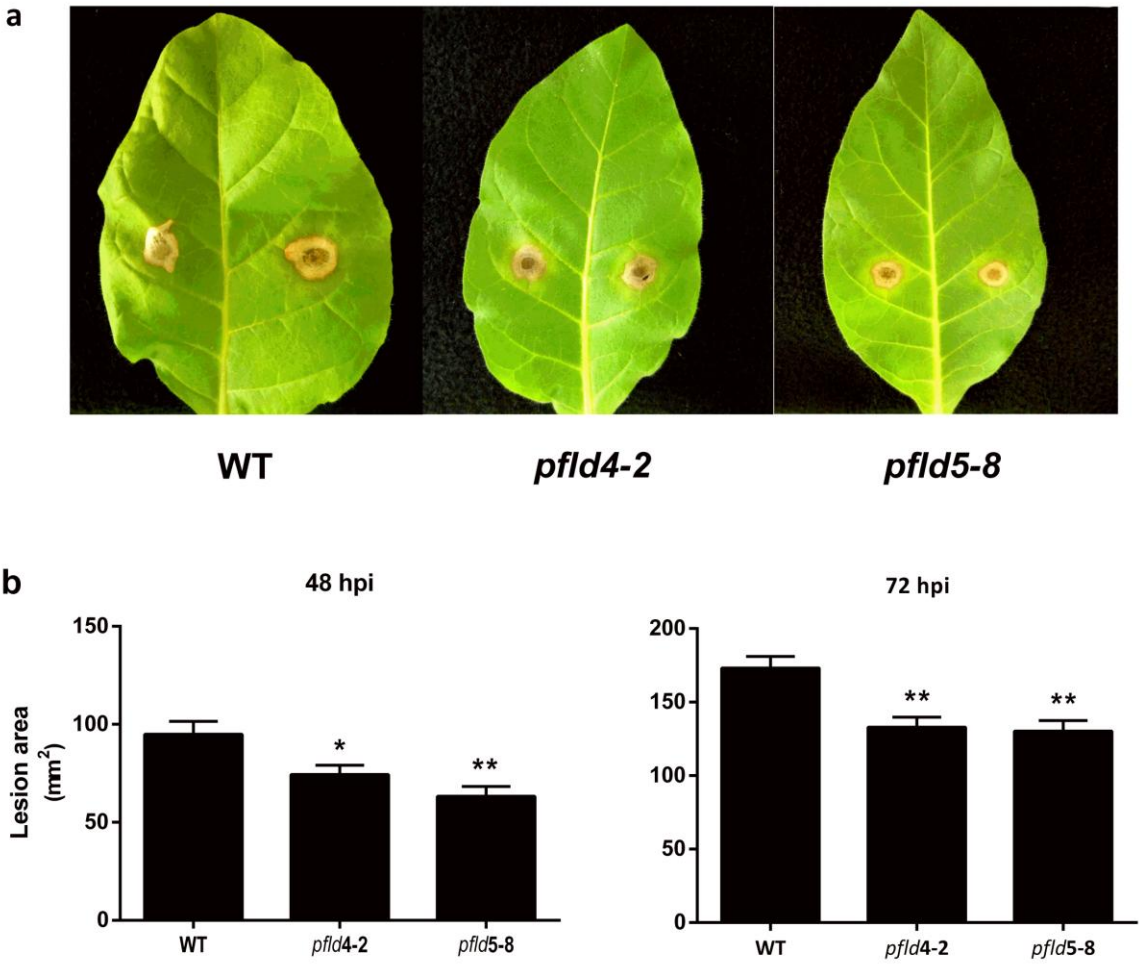

Figure 1. Tissue damage caused by *B. cinerea* infection in WT and transgenic *pfld* lines. Leaves were inoculated with 10 µL of a suspension containing 2.5 x 10^4 conidia on each side of the central vein. (a) Disease symptoms 72 hpi. (b) Sizes of the lesions around the inoculation sites were determined 48 hpi (left) and 72 hpi (right). Results are the means of 5 to 7 replicate leaves ± SD, and statistically significant differences between transgenic and WT plants according to one-way ANOVA and post-hoc comparisons by Dunnet's test are indicated as * ($P \leq 0.05$) and ** ($P \leq 0.01$).

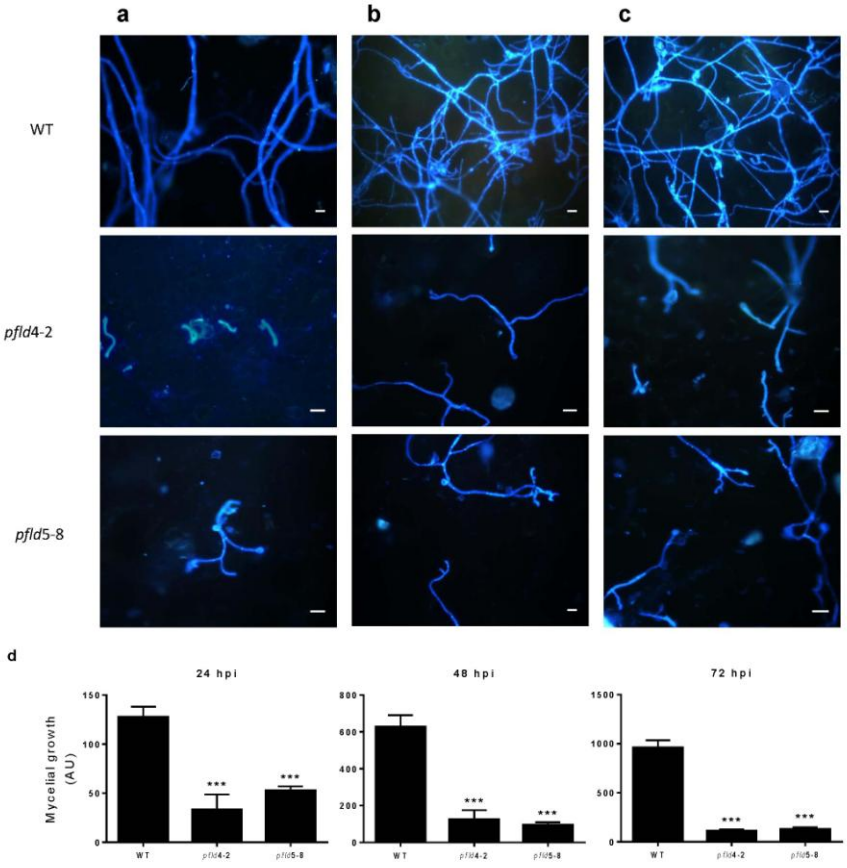

Figure 2. Growth of *B. cinerea* mycelium on leaf discs of WT and *pfld* lines. Discs were inoculated by spreading 10 µL of a suspension containing 1 x 10^5 conidia mL^{-1} with a cotton swab on the adaxial surface. (a-c) Hyphal staining with Calcofluor White 24 hpi (a), 48 hpi (b) and 72 hpi (c) as analyzed by epifluorescence microscopy. Bars = 10 µm. (d) Mycelial growth 24, 48 and 72 hpi. Blue fluorescence intensity is expressed in arbitrary units (AU). Results are means of 3 replicate discs ± SD, and statistically significant differences between transgenic and WT plants according to one-way ANOVA and post-hoc by Dunnett's test are indicated as *** ($P \leq 0.001$).

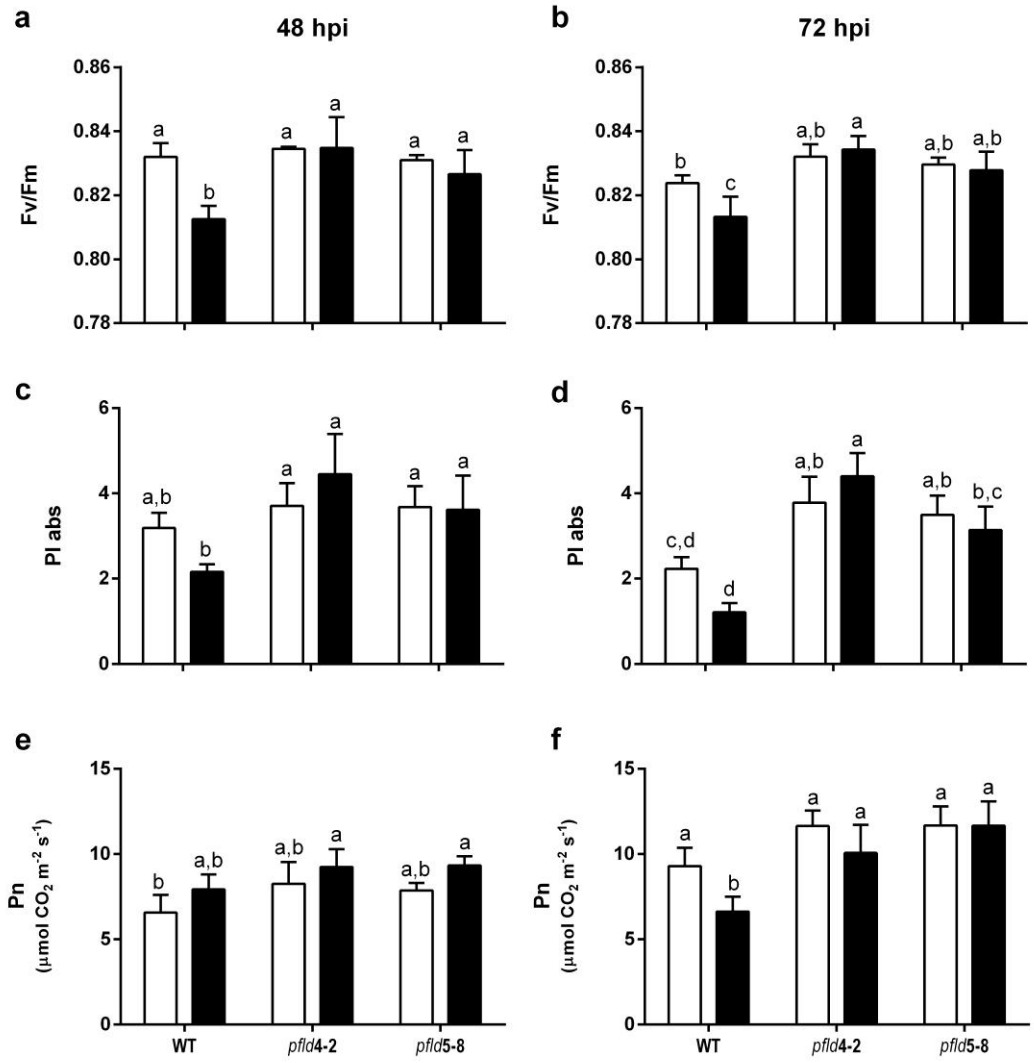

Figure 3. Photosynthetic activities of WT and *pfld* lines infected by *B. cinerea*. Attached leaves were inoculated with 10 µL of a suspension containing 2.5 x 10^4 conidia mL^{-1} on each side of the central vein and plants were incubated during the indicated time-periods within clear plastic boxes to obtain high humidity. Chlorophyll fluorescence parameters were determined in asymptomatic tissues surrounding the lesions (4-5 mm). The maximum quantum efficiency of PSII (Fv/Fm) (a, b), the performance index (PI abs) (c, d) and the maximal CO2 assimilation rate (net photosynthesis = Pn) (e, f) were measured 48 and 72 hpi. White and black bars represent mock- and *B. cinerea*-inoculated plants, respectively. Results are means of 4-5 replicate leaves ± SD, and different letters indicate statistically significant differences ($P \leq 0.05$) between control and infected plants according to two-way ANOVA and Tukey´s post-test.

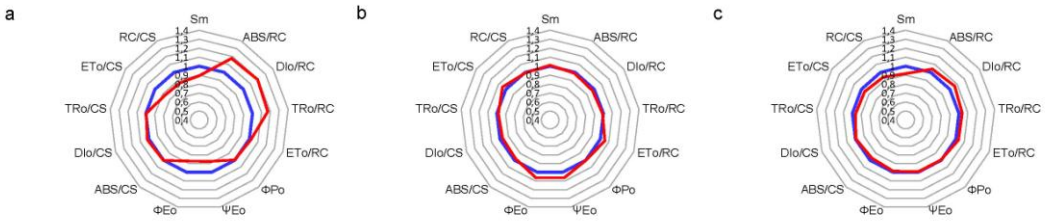

Figure 4. Radar charts of OJIP test parameters determined in WT and *pfld* lines infected with *B. cinerea*. Attached leaves from WT (a), *pfld*4-2 (b) and *pfld*5-8 (c) plants were spot-inoculated with 10 µL of a suspension containing 2.5 x 10^4 conidia mL^{-1} on each side of the central vein and plants were incubated within clear plastic boxes to obtain high humidity. OJIP test parameters were measured in asymptomatic tissues surrounding the lesions 72 hpi. Mean values of 13 OJIP parameters are showed in radar charts for mock (blue lines) and infected (red lines) leaves. Definition of each parameter is provided in Table S1.

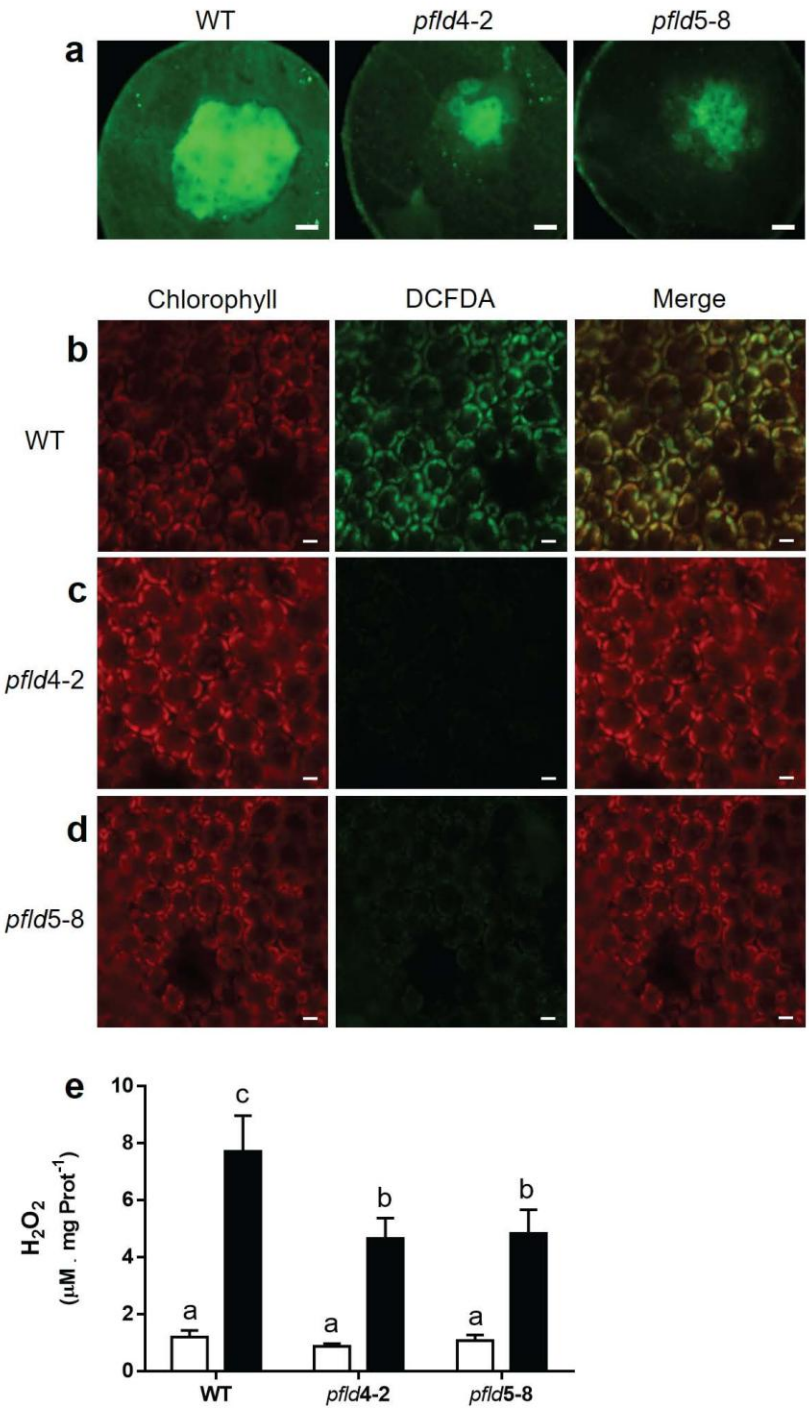

Figure 5. Reactive oxygen species (ROS) accumulation in WT and *pfld* lines infected by *B. cinerea*. *In planta* ROS accumulation was analyzed by fluorescence microscopy after tissue infiltration with DCFDA (a-d). (a) Fluorescence microscopy analysis of ROS accumulation in leaf discs 72 h after spot-inoculation with 10 µL of a suspension containing 2.5 x 10^4 conidia mL^{-1}. Bar = 1 mm. (b-d) Confocal microscopy analysis of subcellular ROS location. Leaf discs were inoculated by spreading 10 µL of a 1 x 10^4 conidia mL^{-1} suspension with a cotton swab. Images show chlorophyll autofluorescence, ROS fluorescence and a merge of chlorophyll and ROS fluorescence for WT (b), *pfld4-2* (c) and *pfld5-8* (d) lines 22 hpi. Bars = 10 µm. (e) Quantification of hydrogen peroxide levels in whole leaf tissue. Leaves were spot-inoculated with 10 µL of a suspension containing 2.5 x 10^4 conidia mL^{-1} on both sides of the central vein and incubated for 72 h. Hydrogen peroxide levels in leaf extracts obtained from tissues adjacent to lesions (4-5 mm) were quantified using the Amplex Red probe. White and black bars represent mock- and *B. cinerea*-inoculated plants, respectively. Results are means of 5 replicate leaves ± SD and different letters indicate statistically significant differences ($P \leq 0.05$) according to two-way ANOVA and Bonferroni's multiple comparison test.

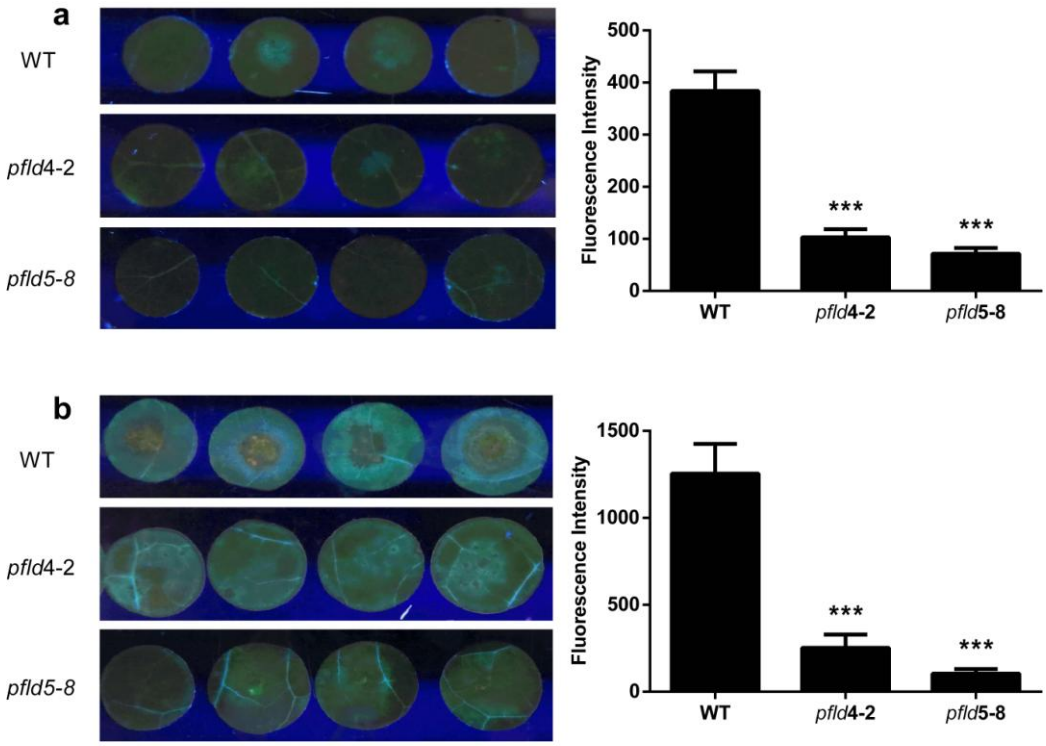

Figure 6. Phytoalexin accumulation in leaf discs of WT and transgenic *pfld* lines infected with *B. cinerea*. Leaf discs were spot-inoculated with 10 µL of a suspension containing 1 x 10^5 conidia mL^{-1} on the adaxial surface. Panels on the left show blue fluorescence due to the accumulation of scopoletin and related compounds in inoculated discs 24 hpi (a) and 48 hpi (b). Panels on the right show the results of fluorescence intensity quantification with the Image J software 24 hpi (a) and 48 hpi (b). Results are means of 5 replicate discs ± SD, and statistically significant differences between control and infected transgenic plants according to one-way ANOVA and Dunnett's test are indicated as *** ($P \leq 0.001$).

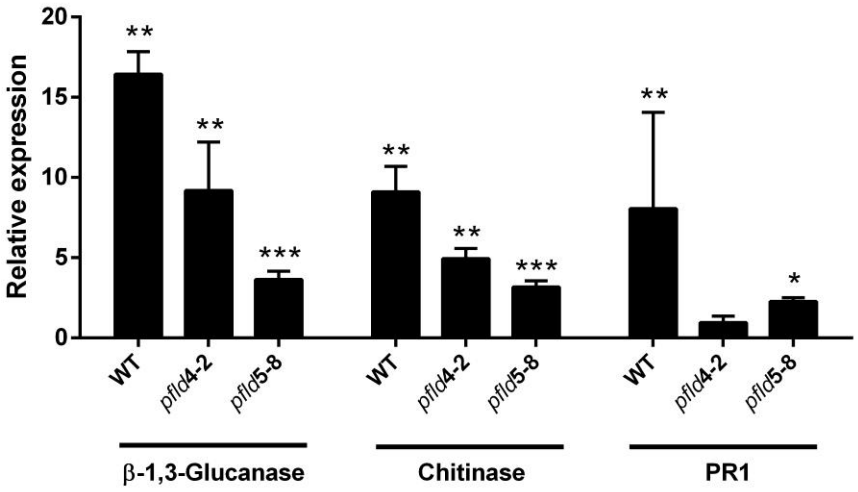

Figure 7. Expression of defense-related genes in WT and transgenic *pfld* lines infected by *B. cinerea*. Droplets (10 µL) of a suspension containing 2.5 x 10^4 conidia mL^{-1} were spot-inoculated on both sides of the central vein and real-time RT-PCR was used to analyse the abundance of gene transcripts 72 hpi. The expression of each gene was normalized to its expression in mock-inoculated plants. Results are means ± SD of 5 replicates and statistically significant differences in gene expression between inoculated and non-inoculated plants of the same line are shown as: * ($P \leq 0.05$), ** ($P \leq 0.01$) and *** ($P \leq 0.001$).